Hot-atom mechanism in photodesorption of molecular oxygen from a stepped platinum (113) surface

Cite as: J. Chem. Phys. **108**, 10231 (1998); https://doi.org/10.1063/1.476483
Submitted: 06 October 1997 . Accepted: 20 March 1998 . Published Online: 10 June 1998

M. Sano, Y. Ohno, T. Yamanaka, T. Matsushima, E. B. Quinay, and K. Jacobi

Hot-atom mechanism in photodesorption of molecular oxygen from a stepped platinum (113) surface

M. Sano, Y. Ohno, T. Yamanaka, T. Matsushima, E. B. Quinay,[a] and K. Jacobi[b]
Graduate School of Environmental Earth Science and Catalysis Research Center, Hokkaido University, Sapporo 060-0811 Japan

(Received 6 October 1997; accepted 20 March 1998)

The photodesorption of oxygen admolecules was studied on a stepped Pt(113)=(*s*)2(111)×(001) surface with 193 nm irradiation at 110 K. Multidirectional desorptions were found to collimate at ±12–20° and ±45–49° off the surface normal and also along the surface normal in a plane along the trough. The first component is always dominant, and the weak second component only appears at higher oxygen coverages. The normally directed desorption is not significant. The translational energy of desorbing O_2 peaks around 15–20° and 50°, confirming the inclined desorptions. It is proposed that these inclined components are due to the desorption induced by the impact of oxygen admolecules with hot oxygen atoms from the photodissociation of adsorbed molecular oxygen, emitted along the trough. A simple cosine distribution was found to fit the thermal desorption from oxygen admolecules and also the recombinative desorption of oxygen adatoms. The 193 nm irradiation also produces additional, less tightly bound oxygen adatoms, which yield a desorption component collimated at 15° from the surface normal in the step-down direction. © *1998 American Institute of Physics.* [S0021-9606(98)02024-8]

I. INTRODUCTION

Surface hot-atoms play an important role in the desorption of coadsorbed species and also in the combinative processes triggered by several photoinduced reactions.[1–6] This paper is the first to report on photodesorption of oxygen admolecules on a stepped Pt(113)=(*s*)2(111)×(001) surface. It delivers ample evidence that the dynamic behavior of hot-atoms can be readily studied on this stepped surface.

The presence of oxygen hot-atoms has been confirmed in stimulated desorptions of coadsorbed species, such as O_2 on Ag(110)[7] and noble gases on Pt(111),[8] and also by studies observing the distribution of thermal- and photolytic-dissociation fragments of oxygen admolecules on Pt(111) with scanning tunneling microscopy (STM).[9,10] The hot-atoms are believed to be emitted parallel to the surface plane because oxygen admolecules are chemisorbed with their axes parallel to the platinum surface plane, except for high coverages below 100 K.[11–15] However, the dynamic behavior of this species is not well understood because its interaction direction is highly variable on the flat surface. Only a tiny O_2 desorption component stimulated by hot oxygen atoms has been found on Ag($\underline{1}$10) around 45° off the normal direction in a plane in the [110] direction. Indeed, most of the photodesorption is collimated along the surface normal. Another inclined O_2 desorption, observed on Pd(111) at the angle of 50–60°, may be due to hot-atoms, but it was explained by a simple photodissociation process of inclined superoxo species.[16,17] On Pt(111), the desorption of coadsorbed noble gases is sharply inclined into the off-normal at around 35°, whereas the photodesorption of O_2 itself and also of the product CO_2 is sharply collimated along the surface normal.[4,18] Thus, at least two desorption channels, one stimulated by hot-atoms and the other without them, seem operative.

Velocity distribution curves of desorbing O_2 frequently involved two components, one with a high translational temperature and the other in a Maxwellian form at the surface temperature. The former was explained by an Antoniewicz repulsive desorption.[19] The latter is due to thermal desorption of O_2 during its photoconversion into a physisorption state or site conversion.[3,20] Their contributions depend on the wavelength and the amount of oxygen adatoms accumulated.[21–23] The translational temperature of desorbing O_2 peaks around the collimation angle, but does not decrease quickly as the angle shifts from this position. It is sometimes much higher than the surface temperature even when the flux distribution approaches a cosine form.[3,7,20] These variations are in contrast with those in the recombinative and repulsive desorption seen in thermal reactions.[24–26] This suggests that several desorption channels are operative in the photoinduced processes.

The desorption induced by the impact of hot-atoms can be expected to be enhanced in a plane along the molecular axis because the atoms are emitted in this direction. Thus, the present surface (see Fig. 1) provides a geometry suitable for examining the momentum transfer into desorbing molecules because its oxygen admolecules lie mostly along the trough.[27] It is a surface where photons induce a reaction between CO and O_2. The two-directional desorption of the product CO_2 was found to be collimated in a plane along the

[a]Also at: Pablo Borbon Memorial Institute of Technology, Rizal Ave., Batngas City, Philippines.
[b]Also at: Fritz-Haber Institute of Max-Planck Society, Faradayweg D-14195, Berlin, Germany.

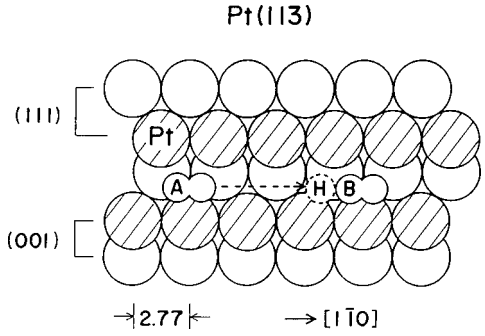

FIG. 1. Structure of the Pt(113) surface and orientation of oxygen admolecules. O_2 (a) is oriented in the trough direction as indicated by A and B. Admolecule A emits hot oxygen atom H that collides with B. The number is in angstrom.

trough.[5] The emission of oxygen hot-atoms was well controlled along the surface trough at low coverage. The oxygen photodesorption was also split into several components inclined in a plane along the trough.

Excitation mechanisms of oxygen admolecules yielding hot-atoms have been examined by the light polarization dependence of desorption and dissociation yields. The results are fairly consistent with a photoexcited carrier mechanism.[28–30] The desorption yield is nonlinearly enhanced with increasing light fluence by a femtosecond-pulsed laser.[31–33] However, no difference has been found in the dynamics of the resultant hot-atoms.

II. EXPERIMENTS

The experimental apparatus consisted of a reaction chamber, a slit chamber, and an analyzer chamber.[34] These were separately evacuated by individual ion pumps. The base pressure was 1×10^{-10} Torr. The reaction chamber had low energy electron diffraction (LEED)—Auger electron spectroscopy (AES) optics, an Ar^+ gun, a quadrupole mass spectrometer, and a gas handling system. The second chamber had a slit on each end. The angle of 2.3° was estimated for a resolution of the acceptance of a second mass spectrometer in the analyzer chamber. The distance from the ionizer of this mass spectrometer to the sample surface at the center of the reaction chamber measured 135 mm. This value was used in calculating the velocity of desorbing species.

A Pt(113) crystal in a disk-shaped slice (10 mm diameter×1 mm thickness, supplied by MaTeck, Germany) was rotated in the reaction chamber to change the desorption angle, θ (polar angle). It was cleaned in the standard cleaning procedure.[34] The irradiation incidence was fixed at 38° against the axis of the mass spectrometer in the analyzer. The angle of irradiation incidence was concomitantly scanned against the surface plane with the desorption angle. The angle of incidence was limited to between $-40°$ and $+40°$ from the bulk surface normal, a range in which the quantum yield of the photodesorption and dissociation was insensitive.[28] The clean surface was exposed to $^{16}O_2$ at 110 K. A nonpolarized ArF laser beam (with a pulse duration of about 16 ns and a fluence of 2 mJ/cm^2 or 1.9×10^{15} photons/pulse) was incident at 5 Hz on the crystal for 6 min in each run. The transient surface temperature rise was estimated to be below 8 K. No thermal effect is believed to have influenced the O_2 desorption and dissociation. The signal due to desorbed $^{16}O_2$ was monitored in angle-resolved form by the mass spectrometer in the analyzer chamber in both photolytic and post-irradiation thermal desorption experiments, and stored in a multichannel scaler (MCS) controlled by a personal computer (PC). The MCS scan and the laser shot were sequentially triggered with a delay pulse generator. The laser power was adjusted while the angle of irradiation incidence was varied so that the flow of photons onto the surface could be kept constant. The surface was flashed to 1000 K after each run. The coverage of oxygen, Θ_{O_2}, was determined by thermal desorption spectroscopy (TDS) in angle-integrated form by using the mass spectrometer in the reaction chamber.[35] The coverage was defined as 1 ML when every Pt atom in the first two layers (see Fig. 1) is occupied by an adspecies.

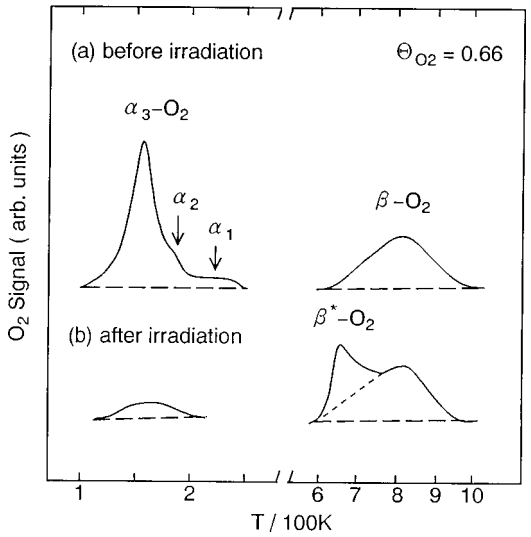

FIG. 2. TDS spectra of (a) α-O_2 and β-O_2 at saturation and (b) after 193 nm irradiation.

III. RESULTS

A. Photodesorption and dissociation

Cross sections for the photodesorption were estimated from post-irradiation TDS and also from the decay of the photodesorption intensity in the surface normal direction. Both showed a first-order process and yielded about $2-8\times10^{-19}$ cm^2. This cross section is reasonable, as compared with 6×10^{-20} cm^2 at 308 nm and 3×10^{-19} cm^2 at 240 nm on Pt(111), because it is consistent with the pattern of increasing value with decreasing wavelength.[18,36]

Typical TDS spectra of oxygen are shown in Fig. 2. The surface was saturated by 1.2 L (Langmuir=1×10^{-6} Torr s) oxygen exposure at 110 K and heated at a rate of 3 K/s below 273 K and 10 K/s above it, before and after laser irradiation. The desorption from the molecular adsorption (α-O_2) peaks in the range of 160–250 K. It consists of three peaks, α_1-O_2 at 220, α_2-O_2 around 185, and α_3-O_2 at 160 K as reported previously.[27] The latter was dominant at saturation and its peak area decreased to about 15% of the initial

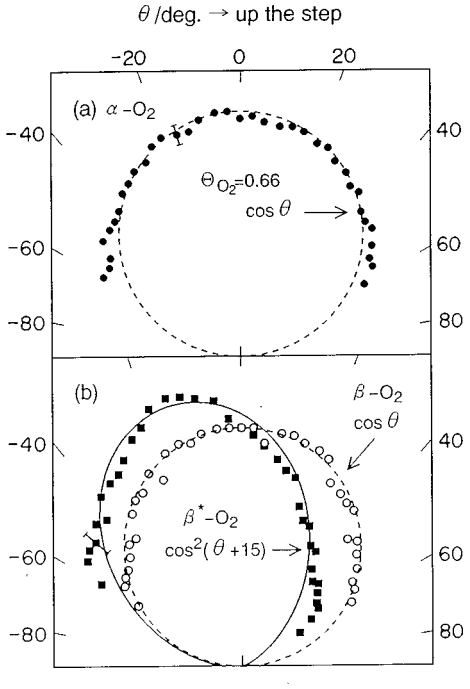

FIG. 3. Angular distributions of (a) α-O_2 desorption, and of (b) β-O_2 and β^*-O_2 desorption in a plane perpendicular to the trough.

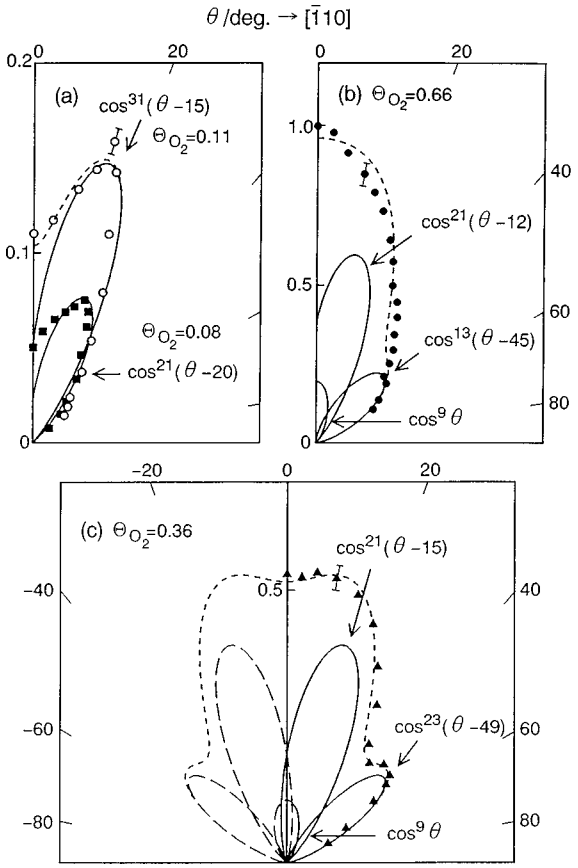

FIG. 4. Angular distributions of oxygen desorbed by 193 nm irradiation in a plane along the trough at various coverages. The solid curves indicate desorption components after a typical deconvolution. The dotted curves show the total flux as the sum of each component (see the text). The distribution for the negative angle range was also drawn at $\Theta_{O_2}=0.36$.

value after 6 min irradiation. Desorption above 600 K (β-O_2), due to the recombination of oxygen adatoms, was accompanied by an additional peak (β^*-O_2) around 680 K after irradiation. This new peak was observed only above $\Theta_{O_2}=0.36$. The increment due to this peak reached about 60% of β-O_2 at saturation. No increase beyond the saturation level was found in β-O_2, even after irradiation.

Oxygen in the β^* state was examined by isotope tracer and the angular distribution of the desorption in post-irradiation TDS. It was differentiated from the oxygen adatoms produced by the thermal dissociation of admolecules. The isotope ^{18}O was highly enriched in the β^* state when the surface covered by $^{16}O(a)$ and $^{18}O_2(a)$ was irradiated at 193 nm. The ^{18}O fraction during the subsequent TDS procedures decreased almost linearly with increasing surface temperature. This indicates that the exchange of oxygen is not fast between the β and β^* states. For any given ^{18}O to ^{16}O ratio, the isotope distribution of O_2 was random.

The angular distributions of oxygen in the above thermally activated desorption processes are summarized in Fig. 3. The α-O_2 desorption always showed a simple cosine distribution in both planes along the trough and perpendicular to it, consistent with a high adsorption probability into the admolecular states.[25,37] A cosine distribution was also found for the β-O_2 desorption with and without irradiation [Fig. 3(b)]. On the other hand, the desorption of oxygen in the β^* state showed a somewhat sharp distribution collimated at 15° off the normal in the step-down direction as $\cos^2(\theta+15)$. This desorption, which is collimated closely along the (001) step normal, suggests that oxygen adatoms produced by irradiation are accumulated on the step sites.

B. Angular distribution in photodesorption

The photodesorption flux of O_2 was determined from time-of-flight (TOF) spectra by considering its velocity. The angular distribution of this flux depended on both the crystal azimuth and the oxygen coverage. Figure 4(a) shows the angular distributions in a plane along the step edge at low coverages. The measurements were performed only in a positive angle range because of the symmetric surface structure with respect to the surface normal in this direction (Fig. 1). The ordinate represents the flux normalized to that in the normal direction at saturation ($\Theta_{O_2}=0.66$). The desorption is collimated around 20° off the surface normal at $\Theta_{O_2}=0.08$. The collimation angle shifted somewhat toward the normal direction with an increase in coverage. Desorption at $\Theta_{O_2}=0.11$ is collimated around $\theta=15°$. The solid curves in Fig. 4(a) show the single-power cosine functions that best fit the data points. The function of $\{\cos(\theta-20)\}^{21\pm2}$ is suitable for the distribution at $\Theta_{O_2}=0.08$, and the form of $\{\cos(\theta-15)\}^{31\pm3}$ is fitted with the data at $\Theta_{O_2}=0.11$. On the other hand, the desorption at high coverage is apparently collimated along the surface normal as shown in Fig. 4(b). In this case, a single-power function of cosine of the desorption angle could not be fitted to the experimental results at $\Theta_{O_2}=0.66$. While a single-power function of $\cos\theta$ can be ap-

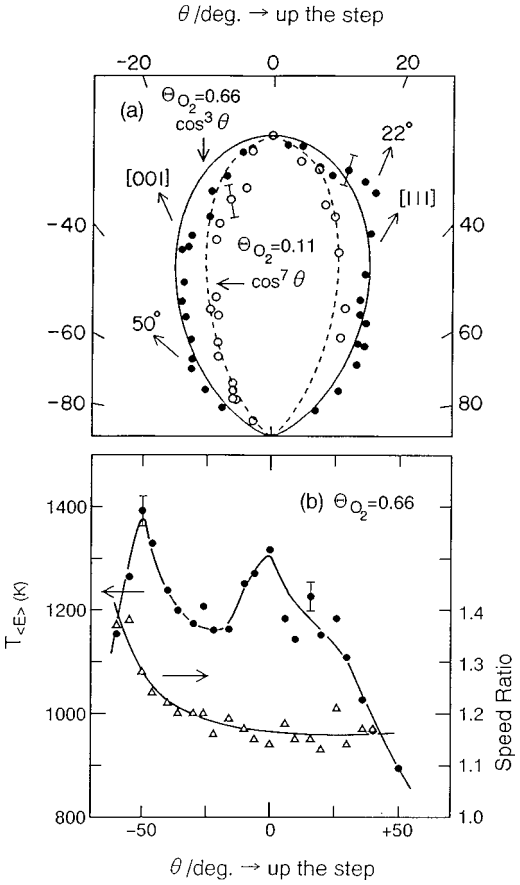

FIG. 5. (a) Angular distributions of oxygen desorbed by 193 nm irradiation in a plane perpendicular to the trough. The flux is normalized to the value in the normal direction for each case. The actual flux at $\Theta_{O_2}=0.11$ was about one ninth of the value at saturation. (b) Variation of the translational energy of desorbing oxygen and the normalized speed ratio with desorption angles.

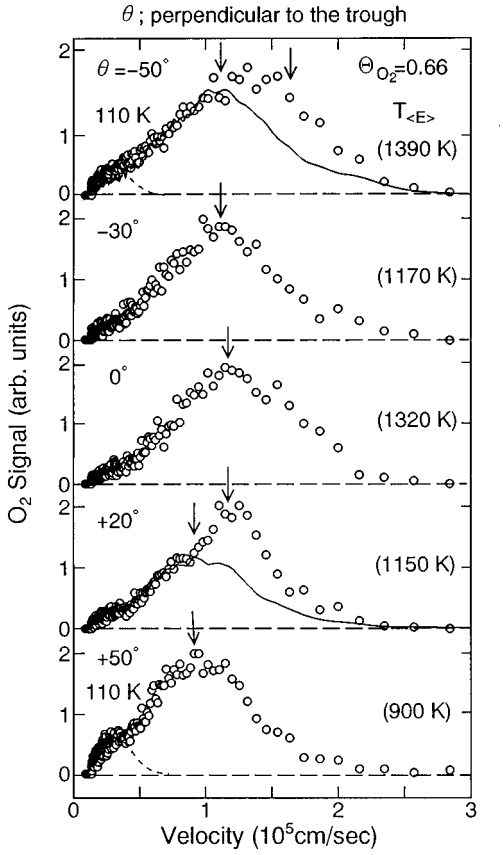

FIG. 6. Velocity distributions of desorbing oxygen at various desorption angles in a plane perpendicular to the trough. The negative sign indicates desorption in the step-down direction. The mean translational energy is shown in parentheses. A Maxwellian distribution at the surface temperature is drawn by the broken curves in the upper and bottom panels. The curve shape for $\theta=-30°$ was inserted in the upper panel for comparison, and also the curve shape for $\theta=+50°$ is shown in the panel at $\theta=+20°$. The downward arrows indicate the peak positions.

plied initially, another component sharply collimated at $\theta=45°$ must be invoked for the remaining flux. This largely inclined desorption is similar to the results yielded by Pd(111) and Ag(110).[7,16,17] This component became clearer at intermediate coverages. The results at $\Theta_{O_2}=0.36$ are shown in Fig. 4(c), where the desorption collimated around 49° is clearly seen. An additional oxygen desorption feature that is detected around $\theta=15-20°$ is also evident.

The angular distribution became simple when the desorption angle was varied in a plane perpendicular to the step edge. The desorption is mostly collimated along the surface normal in a wide coverage range. The desorption was in a $\cos^{6-7}\theta$ form below $\Theta_{O_2}=0.36$. Above this level, it became broad and a small shoulder was found around $+22°$ close to the (111) terrace normal at $+29.5°$, and a smaller bump was observed around $-25°$, close to the (001) step normal. The distributions for $\Theta_{O_2}=0.11$ and 0.66 are shown in Fig. 5(a).

C. Velocity distribution

Velocity measurements of desorbing oxygen were performed to confirm that the above multidirectional desorptions occurred in a plane along the trough. The translational energy was maximized in this plane and its desorption angle dependence was sensitive to the crystal azimuth.

The velocity distribution curves broadened slightly in the course of irradiation, in a way enhancing higher velocity components. This might be caused by the oxygen adatoms produced.[23] The translational temperature ($T_{\langle E\rangle}$), defined as the mean translational energy divided by $2k$ (k is the Boltzmann constant), was plotted as a function of desorption angle in a plane perpendicular to the trough in Fig. 5(b). Two maxima were found in the angle dependence of the energy at $\Theta_{O_2}=0.66$, in the normal direction and around $\theta=-50°$ (in the step-down direction). No peak was found around the (111) terrace and (001) step normals. The velocity distribution curves for $\theta=0°$ and $-50°$ became broad and indicated enhanced higher velocity components, as shown by the downward arrow in the upper panel of Fig. 6. For easier viewing, the curve shape at $\theta=-30°$ was inserted as a solid line. The peak positions of the main component and the slow component were also indicated by arrows. Another desorption component in a Maxwellian form at the surface temperature (shown by the broken curves) became noticeable at large desorption angles, indicating the presence of a diffuse distribution in small amounts. In the end, at least three desorption components must be considered in this direction at high cov-

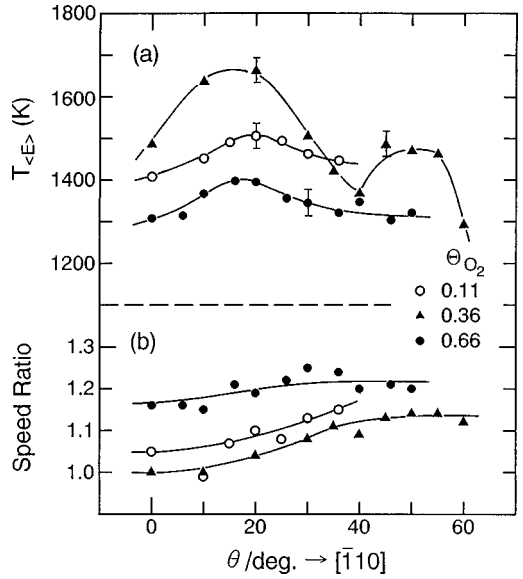

FIG. 7. Variations in (a) the translational energy and (b) the normalized speed ratio at different coverages with desorption angles in a plane along the trough.

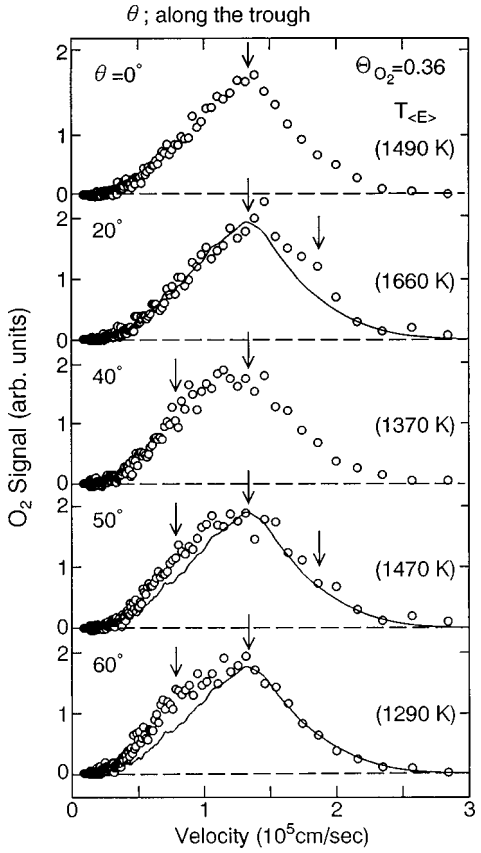

FIG. 8. Velocity distributions of oxygen at various desorption angles in a plane along the trough. The translational energy is shown in parentheses. The curve shape for $\theta=0°$ was inserted in the second, fourth, and fifth panels for comparison. The arrows show the peak position of each component.

erages. However, the velocity curves were not successfully deconvoluted into these components.

The distribution curve was always broad as compared to a Maxwellian form. The normalized speed ratio is defined as $(\langle v^2\rangle/\langle v\rangle^2-1)^{1/2}/(32/9\pi-1)^{1/2}$, where v is the velocity of the molecule, $\langle v\rangle$ is the mean velocity, and $\langle v^2\rangle$ is the mean square velocity. It is unity when the distribution is in a Maxwellian form. The observed value stayed between 1.15 and 1.20 at $\theta=+50°--25°$, as shown in Fig. 5(b). On the other hand, the speed ratio increased steeply from 1.2 to 1.4 as the desorption angle decreased from $\theta=-25°$ to $\theta=-50°$. This suggests an enhanced contribution from a desorption component with high velocities collimated around $-50°$. The flux due to this component, however, must be small because its contribution was hardly noticed in the angular distribution. It should be noted that this collimation angle closely parallels the terrace plane. In the range of $+20-+50°$, on the other hand, the translational energy decreased steeply with increasing desorption angle, suggesting a fast energy dissipation mechanism at large angles in the step-up direction.

The angle dependence of the energy is simple in a plane along the trough, as shown in Fig. 7(a). The translational energy showed a maximum around 20° throughout a wide range of coverages. Additionally, a second maximum was found at around 50° for $\Theta_{O_2}=0.36$. These maxima are consistent with the collimation of the inclined desorptions in this plane. It should be noticed that the energy was generally higher than that perpendicular to the trough. This also supports that the desorption is collimated in this plane. Furthermore, the energy at saturation was less than that at lower coverages, suggesting an energy dissipation by collisions with admolecules.

An attempt to deconvolute the velocity distributions into components was again not successful, despite the fact that the curves were always broad and hinted at the presence of three components. The observed speed ratio was rather constant around 1.2 at saturation over a wide range of angles, as shown in Fig. 7(b). At $\Theta_{O_2}=0.36$, the value increased from unity in the normal direction to 1.14 at $\theta=50°$. Typical velocity distributions at $\Theta_{O_2}=0.36$ in a plane along the trough are summarized in Fig. 8. The distribution curve at $\theta=0°$ showed a sharp decay of the signal in the velocity region above the maximum. This curve can not be simulated by any single modified Maxwellian form. For a comparison, the curve shape at $\theta=0°$ was inserted into the second panel for $\theta=20°$. An enhancement of the signal is seen in velocities above the maximum position, as indicated by the downward arrow. The signal above the maximum decreased once around $\theta=+40°$, after which it again increased around $\theta=+50°$. This is consistent with the presence of the desorption components collimated around this angle. The slow component below the maximum was enhanced at large desorption angles.

IV. DISCUSSION

A. Desorption channels

Under ultraviolet irradiation, chemisorbed oxygen molecules undergo photodesorption, photodissociation, and also sometimes photorearrangements.[38–40] All these processes are usually believed to result from the transient capture of a pho-

toexcited substrate electron into the unfilled $3\sigma_u^*$ orbital of the admolecule. This short-lived $O_2^-(a)$ dissociates, or is moved toward the surface by the image force and then neutralized. The resultant neutral O_2 will receive a repulsive force in close proximity to the metal surface. This may result in a translationally and vibrationally excited neutral molecule, which can desorb or dissociate.

In this Antoniewicz bounce mechanism, the desorption must be collimated along the normal direction of the adsorption site because the repulsive force due to the Pauli repulsion is exerted toward the neutral O_2 from the surface. In fact, the O_2 photodesorption is mostly collimated along the bulk surface normal on the flat surfaces of Pt(111), Ag(110), and Pd(111).[3,7,20] However, the translational temperature does not decrease quickly toward the surface value with increasing desorption angle. There must, therefore, be a mechanism whereby the repulsive force is operative along the inclined direction. Such inclined desorption can be concentrated on the present surface into a plane along the trough. The desorption flux and the translational energy show two maxima in their angle dependence in this plane in the positive angle range, confirming the inclined desorptions. Furthermore, no maximum in translational energy is found in the normal direction. Thus, the normally directed component, if present at all, is not significant and its energy is substantially less than that of the inclined component.

A result of the symmetry of this surface and the presence of these inclined desorption components is that the desorption is split in a multidirectional way collimated at $\pm 12-20°$ and $\pm 45-49°$ in a plane along the trough. These off-normal desorptions can be reasonably expected on the present surface because oxygen admolecules, which lie along the surface plane and are oriented parallel to the step edges, emit hot-atoms along their axes.[27]

B. Collimation angle

The collimation angle of the inclined desorption depends on the coverage. The desorption is collimated around 20° at $\Theta_{O_2}=0.08$ and is shifted to 15° at $\Theta_{O_2}=0.11$. This angle continues to shift somewhat with increasing coverage. At saturation, it was estimated to be 12° as shown below. The best deconvolutions are shown by the solid curves in Figs. 4(b) and 4(c). The deconvolution was performed under conditions where each desorption component was approximated by a single-power function of the cosine of the desorption angle and is collimated around the angle where the translational energy is maximized. Only the two components collimated at $\theta=15$ and 49° are capable of simulating most of the observed flux at $\Theta_{O_2}=0.36$. The normally directed desorption contributes only in a small amount, as shown by the solid curve in a form of $\cos^9(\theta)$. The dotted curve in Fig. 4(c) indicates the total flux calculated as $0.41\cos^{21}(\theta-15)+0.41\cos^{21}(\theta+15)+0.24\cos^{23}(\theta-49)+0.24\cos^{23}(\theta+49)+0.12\cos^9(\theta)$. The drawing in the negative angle range (shown by broken curves) is based on the surface symmetry. The dotted curve in Fig. 4(a) was drawn as $0.15\cos^{31}(\theta-15)+0.15\cos^{31}(\theta+15)$.

On the other hand, a unique deconvolution was not successful at saturation. Remaining flux at saturation after subtraction of a $\cos^{13}(\theta-45)$ component was fitted the sum of two components of $\cos^{21}(\theta-12)$ and $\cos^9(\theta)$ forms. The results in Fig. 4(b) were obtained at the maximum contribution of the inclined component. The dotted line was drawn as $0.61\cos^{21}(\theta-12)+0.61\cos^{21}(\theta+12)+0.3\cos^{13}(\theta-45)+0.3\cos^{13}(\theta+45)+0.19\cos^9(\theta)$. The inclined component at $\theta=\pm 12°$ may be somewhat overestimated.

A rather broad angular distribution was frequently reported in the photodesorption of chemisorbed $O_2(a)$ on Pt(111) and Pd(111), although the average kinetic energy is much higher than that expected from a Maxwellian distribution at the surface temperature.[3,20] This broad distribution is largely due to the contribution of the inclined components. In fact, the distribution in a plane perpendicular to the trough is sharp ($\cos^{6-7}\theta$) at low coverage and confirms that the multidirectional desorption is limited in a plane along the trough. At saturation, the distribution is broad, as approximated in a $\cos^3\theta$ form. It should be compared with the sharper distribution in a plane along the trough. This anisotropy is apparently opposite in the repulsive desorption of the product CO_2 since its distribution along the trough is always broader than that perpendicular to it.[26] This tends to support the notion that the desorption in this case is not collimated along the surface normal.

The above angular distribution is different from that of the product CO_2 in the photolytic CO oxidation, where the CO_2 desorption is sharply collimated to the (111) terrace normal, the (001) step normal, and also the bulk surface normal at high O_2 coverage.[6,41] The translational energy of the CO_2 is much higher than that of O_2. A different desorption mechanism can therefore be expected in the CO photooxidation.

C. Admolecule participation

The orientation of oxygen admolecules was examined by NEXAFS (near-edge x-ray absorption fine structure) on platinum surfaces with declining terraces, such as Pt(113),[27] $Pt(110)(1\times 2)$,[42] and $Pt(133)=(s)3(111)\times(111)$.[43] On these surfaces, oxygen admolecules are commonly oriented along the trough at low coverages. Such molecules (named α_1-O_2) have a rather high adsorption energy and are suppressed completely by preadsorption of oxygen adatoms. At higher coverages, other admolecules (α_2-O_2 and α_3-O_2) with lower adsorption energies still orient fairly along the trough on Pt(113). Recent STM work on Pt(111) shows that O_2 admolecules are located on bridge and face-centered-cubic (fcc) hollow sites at low coverages and also on bridge sites of the upper terrace on (111) micro-facets, but not on steps with (001) micro-facets.[10] Thus, it is likely that α_1-O_2 is on one of the fcc hollow sites which orients the molecular axis parallel to the trough, as drawn in Fig. 1. α_2-O_2 and α_3-O_2 may be distributed on a terrace close to the trough, or near α_1-O_2 on the upper terrace. All these admolecules may contribute the Antoniewicz desorption collimated along the (111) terrace normal. However, such desorption was found at high coverages only as a small shoulder around $\theta=+22°$ in the step-up direction.

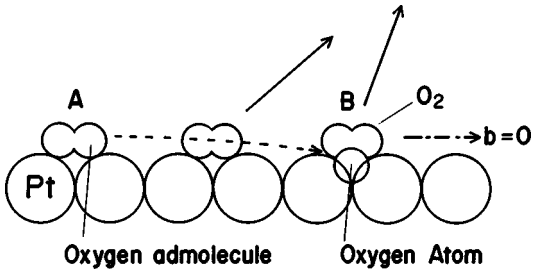

FIG. 9. A hot-atom collision mechanism. The desorption is collimated along different angles depending on the distance between adsorbates.

The photodesorption seems to be mostly induced by the momentum transfer of hot-atoms emitted from oxygen admolecules. The Antoniewicz desorption model does not explain the inclined components because the surface is rather flat along the trough and no oriented facets are found. The oxygen desorption through the collision channel is hardly noticed on flat Pt(111) because admolecules are oriented in several directions and hot-atoms are emitted in a wide range of angles parallel to the surface plane.[3]

D. Hot-atom energy

The maximum translational energy of O_2 involved in desorption by hot-atoms was estimated at around 1.0 eV from maximum velocity of about 2.5×10^5 cm/s. The energy of hot-atoms must be partly used to break the O_2–metal bond. At low coverages, only α_1-O_2 contributes to the desorption. The dissociation energy of this bond is about 0.6 eV for α_1-O_2.[27] The hot-atom can be expected to originally have the lower bound energy of 1.6 eV. This value should be compared with the energy of 0.73 eV estimated by Harrison[3] for hot oxygen atoms on Pt(111) at 250 nm irradiation. The value in the present case is higher, probably because of the usage of a shorter wavelength irradiation.

E. Collision desorption

The presence of several collimation angles can be predicted in a qualitative way by a hard sphere inelastic collision as sketched in Fig. 9. The desorption of oxygen molecules should be collimated at the angle of $\theta=\cos^{-1}(b/d)$ where b is the impact parameter and d is the collision diameter.[44] The latter is the sum of the radius of O_2 and oxygen hot-atoms and is roughly estimated as 2.1 Å.[45]

The impact parameter in this system would be small when hot-atoms are emitted and collide with neighboring oxygen admolecules, keeping the distance from the surface constant (head-on collision; $b=0$). The resultant desorption should be collimated closely to the surface plane. However, this is not the case in the plane along the trough. Nevertheless, the desorption around $\theta=-50°$ in the step-down direction may be explained in such a collision desorption, because its collimation angle closely parallels the terrace plane, and oxygen may be populated there at high coverages. In this mechanism, oxygen admolecules emitting hot-atoms should lie on the terrace and their axis should be considerably rotated from the trough direction. Such oriented oxygen was proposed by NEXAFS study[27,43] and recent STM work.[10] Of course, a simple photodesorption of inclined admolecules can explain this desorption component when their axis orients at $\theta=-50°$.[16]

The collimation angles of 12–20° and 45–49° require impact parameters of $b=\sim2.0$ and ~1.4 Å. These values are not unreasonable because the admolecule seems to be located further from the surface,[46] and oxygen adatoms are 0.85 Å above the platinum plane.[47] This consideration suggests that hot-atoms are moved toward the surface as well as along the trough, as expected due to the attractive force needed to yield a strong oxygen–metal bond (about 3.7 eV).[48] At high coverage, collision with smaller impact parameters becomes possible because the distance between neighboring admolecules becomes shorter and the resultant desorption must be collimated at larger desorption angles. This explains the component with the large impact parameter in a wide coverage range and the other with the smaller only at high coverages. For example, when the aligned molecules form strings,[10] the collimation at 45–49° may correspond to the impact at the second nearest site and the other at the third nearest site. Of course, the collimation angle would be decreased and the above impact parameters would be overestimated when the repulsive force is operative toward O_2, desorbing from the surface just after the breaking of the O_2–metal bond.

Poor energy transfer from a hot-atom to desorbing O_2 is expected in the above simple mechanism because heavy O_2 moving along inclined directions can not efficiently receive the kinetic energy during a single collision event, especially at small collimation angles.[44] However, the desorbing O_2 held a high kinetic energy. This is reminiscent of noble gasses desorbed by hot-atom collision on Pt(111).[3,4] Another energy transfer channel may be invoked in this desorption event, in which significant energy, except the kinetic form of hot-atoms, is released probably in the subsequent oxygen–metal bond formation. In fact, recent atom beam experiments indicate that oxygen admolecules are repulsively desorbed by supplying oxygen atoms onto the surface.[21,49] Rettner and Lee proposed that the desorption may result from changes in the local surface electronic structure due to the formation of a new platinum–adatom bond, thus withdrawing charge from molecular oxygen on the surface and leaving it high on the repulsive potential. This may contribute to the shift of the collimation angle toward the surface normal, and also enhance the kinetic energy of oxygen. The lower bound energy of hot-atoms, estimated in the former section, may be overestimated when this mechanism works well.

V. SUMMARY

Photodesorption of oxygen admolecules was studied on Pt(113) by using an ArF excimer laser. The results are summarized as follows:

(1) Oxygen adatoms produced by photodissociation are likely to accumulate at (001) step sites at high coverage.
(2) A multidirectional desorption, collimated at $\pm12-20°$ and $\pm45-49°$ off the surface normal, is found in a plane along the trough. The normally directed component is not significant.

(3) The inclined components are reasonably well explained by collision-induced desorption with hot-atoms emitted from oxygen admolecules oriented along the trough.

ACKNOWLEDGMENTS

M. Sano is grateful for the support from the Sasakawa Scientific Research Grant from the Japan Science Society. E. B. Quinay is indebted to Japan International Cooperation Agency (JICA) for support received through the Catalytic Science Group Training Course. K. Jacobi acknowledges the support he received through the foreign researcher (COE) invitation program in 1996 by the Ministry of Education, Science, Sport and Culture of Japan. This work was also supported in part by Grant-in-Aid No. 06403012 for Scientific Research (A) from the above Ministry.

[1] W. D. Mieher and W. Ho, J. Chem. Phys. **91**, 2755 (1989).
[2] T. A. Germer and W. Ho, J. Chem. Phys. **93**, 1474 (1990).
[3] I. Harrison, V. A. Ukraintsev, and A. N. Artsyukhovich, SPIE Proc. **2125**, 285 (1994).
[4] A. N. Artsyukhovich and I. Harrison, Surf. Sci. **350**, L199 (1996).
[5] T. Yamanaka, Y. Inoue, and T. Matsushima, Chem. Phys. Lett. **264**, 180 (1997).
[6] T. Yamanaka, Y. Inoue, M. Sano, C. Moise, and T. Matsushima, Appl. Surf. Sci. **121/122**, 601 (1997).
[7] Q.-S. Xin and X.-Y. Zhu, Surf. Sci. **347**, 346 (1996); X. Y. Zhu, *ibid.* **390**, 224 (1997).
[8] I. Harrison, Proc. Oji Seminar, edited by K. Tanaka (Word Publishing House, Tokyo, 1996), p. 35.
[9] J. Wintterlin, R. Schuster, and G. Ertl, Phys. Rev. Lett. **77**, 123 (1996).
[10] B. C. Stipe, M. A. Rezaei, W. Ho, S. Gao, M. Persson, and B. I. Lundguist, Phys. Rev. Lett. **78**, 4410 (1997); B. C. Stipe, M. A. Rezaei, and W. Ho, J. Chem. Phys. **107**, 6443 (1997).
[11] J. Stöhr, J. L. Gland, W. Eberhardt, D. A. Outka, R. J. Madix, F. Sette, R. J. Koestner, and U. Doebler, Phys. Rev. Lett. **51**, 2414 (1983); W. Wurth, J. Stöhr, P. Feulner, X. Pan, K. R. Bauchspiess, Y. Baba, E. Hudel, G. Rocker, and D. Menzel, *ibid.* **65**, 2426 (1990).
[12] D. A. Outka, J. Stöhr, W. Jark, P. Stevens, J. Solomon, and R. J. Madix, Phys. Rev. B **35**, 4119 (1987).
[13] J. L. Gland, Surf. Sci. **93**, 487 (1980).
[14] H. Steininger, S. Lehwald, and H. Ibach, Surf. Sci. **123**, 1 (1982).
[15] J. Schmidt, Ch. Stuhlmann, and H. Ibach, Surf. Sci. **284**, 121 (1993).
[16] A. de Meilere, H. Hirayama, and E. Hasselbrink, Phys. Rev. Lett. **70**, 1147 (1993).
[17] A. de Meijere, H. Hirayama, F. Weik, and E. Hasselbrink, *Desorption Induced by Electron Transitions DIET V*, edited by A. R. Burns, E. B. Stechel, and D. R. Jennison (Springer-Verlag, Berlin, 1993), p. 57.
[18] V. A. Ukraintsev and I. Harrison, J. Chem. Phys. **96**, 6307 (1992).
[19] P. R. Antoniewicz, Phys. Rev. B **9**, 3811 (1980).
[20] E. Hasselbrink, H. Hirayama, A. de Meijere, F. Weik, M. Wolf, and G. Ertl, Surf. Sci. **269/270**, 235 (1992).
[21] C. T. Rettner and J. Lee, J. Chem. Phys. **101**, 10 185 (1994).
[22] F. Weik, A. de Meijere, and E. Hasselbrink, J. Chem. Phys. **99**, 682 (1993).
[23] M. Wolf, E. Hasselbrink, J. M. White, and G. Ertl, J. Chem. Phys. **93**, 5327 (1990).
[24] G. Comsa and R. David, Surf. Sci. Rep. **5**, 145 (1985).
[25] G. Ehrlich, *Chemistry and Physics of Solid Surfaces*, edited by R. Vancelow and R. Howe (Springer-Verlag, Berlin 1988), Vol. VII, p. 1.
[26] T. Matsushima, Heterog. Chem. Rev. **2**, 51 (1996).
[27] T. Yamanaka, T. Matsushima, S. Tanaka, and M. Kamada, Surf. Sci. **349**, 119 (1996).
[28] X.-Y. Zhu, J. M. White, M. Wilf, E. Hasselbrink, and G. Ertl, Chem. Phys. Lett. **176**, 459 (1991).
[29] M. Wolf, E. Hasselbrink, G. Ertl, X.-Y. Zhu, and J. M. White, Surf. Sci. **248**, L235 (1991).
[30] S. R. Hatch, X.-Y. Zhu, J. M. White, and A. Campion, J. Phys. Chem. **95**, 1759 (1991).
[31] S. Deliwala, R. J. Finay, J. R. Goldman, T. H. Her, W. D. Mieher, E. Mazur, Chem. Phys. Lett. **242**, 617 (1995).
[32] F.-J. Kao, D. G. Busch, D. Gomes da Costa, and W. Ho, Phys. Rev. Lett. **70**, 4098 (1993); F.-J. Kao, D. G. Busch, D. Cohen, D. Gomes da Costa, and W. Ho, *ibid.* **71**, 2094 (1993).
[33] J. A. Misewich, A. Kalamarides, T. F. Heinz, U. Höfer, and M. M. T. Loy, J. Chem. Phys. **100**, 736 (1994).
[34] T. Matsushima, Surf. Sci. **127**, 403 (1983).
[35] T. Yamanaka, C. Moise, and T. Matsushima, J. Chem. Phys. **107**, 8138 (1997).
[36] W. D. Mieher and W. Ho, J. Chem. Phys. **99**, 9279 (1993).
[37] W. van Willigen, Phys. Lett. **28A**, 80 (1968).
[38] X. Guo, L. Hanley, and J. T. Yates, Jr., J. Chem. Phys. **90**, 5200 (1989); L. Hanley, X. Guo, and J. T. Yates, Jr., *ibid.* **91**, 7220 (1989).
[39] X.-Y. Zhu, S. R. Hatch, A. Campion, and J. M. White, J. Chem. Phys. **91**, 5011 (1989).
[40] S. R. Hatch, X.-Y. Zhu, J. M. White, and A. Campion, J. Chem. Phys. **92**, 2681 (1990).
[41] T. Matsushima, T. Yamanaka, and Y. Ohno, Sci. Rep. Res. Inst. Tohoku Univ. A **44**, 215 (1997).
[42] Y. Ohno, T. Matsushima, S. Tanaka, E. Yagasaki, and M. Kamada, Surf. Sci. **275**, 281 (1992).
[43] M. Sano, Y. Seimiya, Y. Ohno, T. Matsushima, S. Tanaka, and M. Kamada, Appl. Surf. Sci. (in press).
[44] J. B. Hasted, *Physics of Atomic Collisions* (Butterworth, London, 1964), p. 41.
[45] W. E. Forsythe, *Smithsonian Physical Tables*, 9th ed. (Smithsonian Institution, Washington, 1959), p. 643.
[46] L. Vaska, Acc. Chem. Res. **9**, 175 (1976).
[47] K. Mortensen, C. Klink, F. Jensen, F. Besenbacher, and I. Stensgaard, Surf. Sci. **220**, L701 (1989).
[48] C. T. Campbell, G. Ertl, H. Kuippers, and J. Segner, Surf. Sci. **107**, 220 (1981).
[49] M. C. Wheeler, D. C. Seets, and C. B. Mullins, J. Chem. Phys. **107**, 1672 (1997).